

See discussions, stats, and author profiles for this publication at: <https://www.researchgate.net/publication/263940395>

# Preparation of Low Band Gap Fibrillar Structures by Solvent-Induced Crystallization

ARTICLE in ACS MACRO LETTERS · DECEMBER 2013

Impact Factor: 5.76 · DOI: 10.1021/mz400431s

---

CITATIONS

10

---

READS

34

4 AUTHORS, INCLUDING:



Hsin-Wei Wang

University of Massachusetts Amherst

9 PUBLICATIONS 125 CITATIONS

SEE PROFILE



Emily Pentzer

Case Western Reserve University

20 PUBLICATIONS 191 CITATIONS

SEE PROFILE

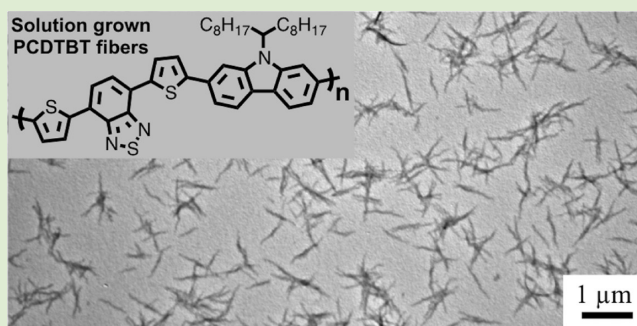
# Preparation of Low Band Gap Fibrillar Structures by Solvent-Induced Crystallization

Hsin-Wei Wang, Emily Pentzer,<sup>†</sup> Todd Emrick,\* and Thomas P. Russell\*

Polymer Science and Engineering Department, University of Massachusetts, Amherst, Massachusetts 01003, United States

**S** Supporting Information

**ABSTRACT:** Solvent-induced crystallization of the low band gap polymer poly[*N*-9"-heptadecanyl-2,7-carbazole-alt-5,5-(4',7'-di-2-thienyl-2',1',3'-benzothiadiazole)] (PCDTBT) was shown to give fibril-like structures of 40–60 nm width and ~0.5  $\mu\text{m}$  length. These structures, formed by heating and cooling PCDTBT in a marginal solvent for the polymer, were characterized by AFM, TEM, GI-WAXS, and steady state absorption and emission spectroscopy. The width of the PCDTBT structures suggests that the polymer chains are oriented perpendicular to the fiber axis, while the observed undulated structure, as revealed by AFM, suggests that the nanostructures may be composed of smaller crystalline units that associate preferentially on specific faces of the crystals. The spectroscopic signatures of the suspended PCDTBT fibrils resembled that of the polymer in solution, in contrast to features associated with the fibril formation of the well-known conjugated polymer poly(3-hexyl thiophene) (P3HT). The solution-based crystallization of PCDTBT reported herein offers insight into the self-assembly of conjugated polymers toward better understanding of their role in photovoltaic devices.



Well-defined nanostructures prepared from conjugated polymers are desirable for numerous electronically active devices, including solar cells.<sup>1,2</sup> In typical bulk heterojunction devices (BHJ) based on poly(3-hexylthiophene) (P3HT) and phenyl- $\text{C}_{61}$ -butyric acid methyl ester ( $\text{PC}_{61}\text{BM}$ ), crystallization of P3HT can enhance device performance. Improved  $\pi$ – $\pi$  stacking and chain ordering in the P3HT phase balances charge mobility between  $\text{PC}_{61}\text{BM}$  and P3HT, and increases power conversion efficiency (PCE) of devices.<sup>3</sup> However, the formation of crystalline order in the active layer depends strongly on processing conditions, including solubility of P3HT and  $\text{PC}_{61}\text{BM}$  in the solvent(s), additives used to control solubilization of the components,<sup>4,5</sup> solvent evaporation rate,<sup>6</sup> and thermal or solvent annealing treatments of the resultant film. Recently, well-defined crystalline P3HT fibrils were formed in solution and used in the active layer of BHJ solar cells.<sup>7,8</sup> Deposition of these preformed crystalline P3HT fibrils as blends with an electron acceptor precludes the need for postprocessing treatments to induce polymer crystallization.<sup>9–12</sup> Such fibrils offer a higher charge mobility relative to amorphous P3HT and provide a unique opportunity to investigate new designs and fabrication methods of solar cells, like the controlled assembly of the fibrils or nanowires with electron acceptors<sup>11,13</sup> and stabilization of fibrillar nanostructures through cross-linking.<sup>14</sup>

Ideally, principles underpinning the solution-based crystallization of P3HT will be applicable to low bandgap polymers, which provide a broader absorption of the solar spectrum. However, reports to date on the morphology of low band gap polymers or their crystallization from solution are very

limited.<sup>15,16</sup> Here, we report a simple solution-based preparation of crystalline, nanoscale polymer fibrils from the low bandgap polymer, poly[*N*-9"-heptadecanyl-2,7-carbazole-alt-5,5-(4',7'-di-2-thienyl-2',1',3'-benzothiadiazole)] (PCDTBT). These solution-formed PCDTBT fibrils were characterized by transmission electron microscopy (TEM), atomic force microscopy (AFM), grazing-incidence wide-angle X-ray scattering (GI-WAXS), and steady-state absorption and fluorescence emission spectroscopies. PCDTBT was chosen since it exhibits very high internal quantum efficiency,<sup>17</sup> has an estimated operating lifetime of >6 yr,<sup>18</sup> and as an active layer component in devices leads to 6–7% PCE, typically surpassing the PCE of P3HT-based devices.<sup>19</sup> The relatively high glass transition temperature ( $T_g$ ) of PCDTBT (~130  $^{\circ}\text{C}$ ) and the rigidity of the chain suggest that thermal annealing at elevated temperature, or extended time periods, would induce crystallization in thin films.<sup>20</sup> Yet, decreased PCEs are observed for annealed devices containing an active layer of PCDTBT/ $\text{PC}_{71}\text{BM}$ , likely due to coarsening of  $\text{PC}_{61}\text{BM}$  aggregates<sup>21</sup> and a decreased coherence length of the  $\pi$ -stacked chains<sup>22</sup> that disrupts the electronic structure of the polymer.

PCDTBT was synthesized by Suzuki polymerization of 2,7-bis(4',4',5',5'-tetramethyl-1',3',2'-dioxaborolan-2'-yl)-*N*-9"-heptadecanylecarbazole and 4,7-di(2'-bromothiophen-5'-yl)-2,1,3-benzothiadiazole, as previously reported.<sup>23</sup> Two polymer

Received: August 16, 2013

Accepted: December 6, 2013

Published: December 17, 2013



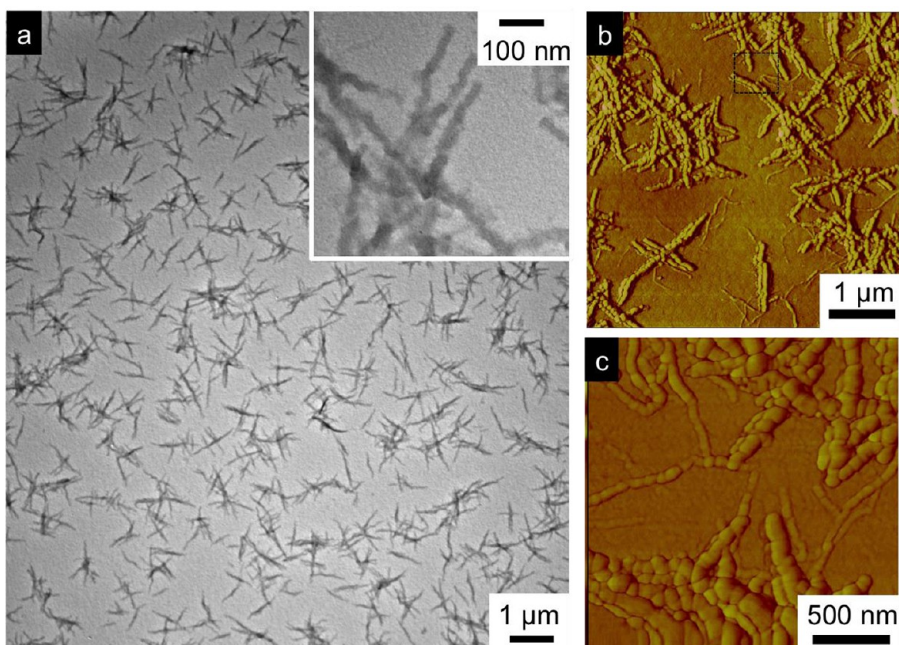


**Figure 1.** (a) TEM image of PCDTBT fibrils; (b) AFM phase image of PCDTBT fibrils; and (c) higher magnification AFM phase image of fibrils.

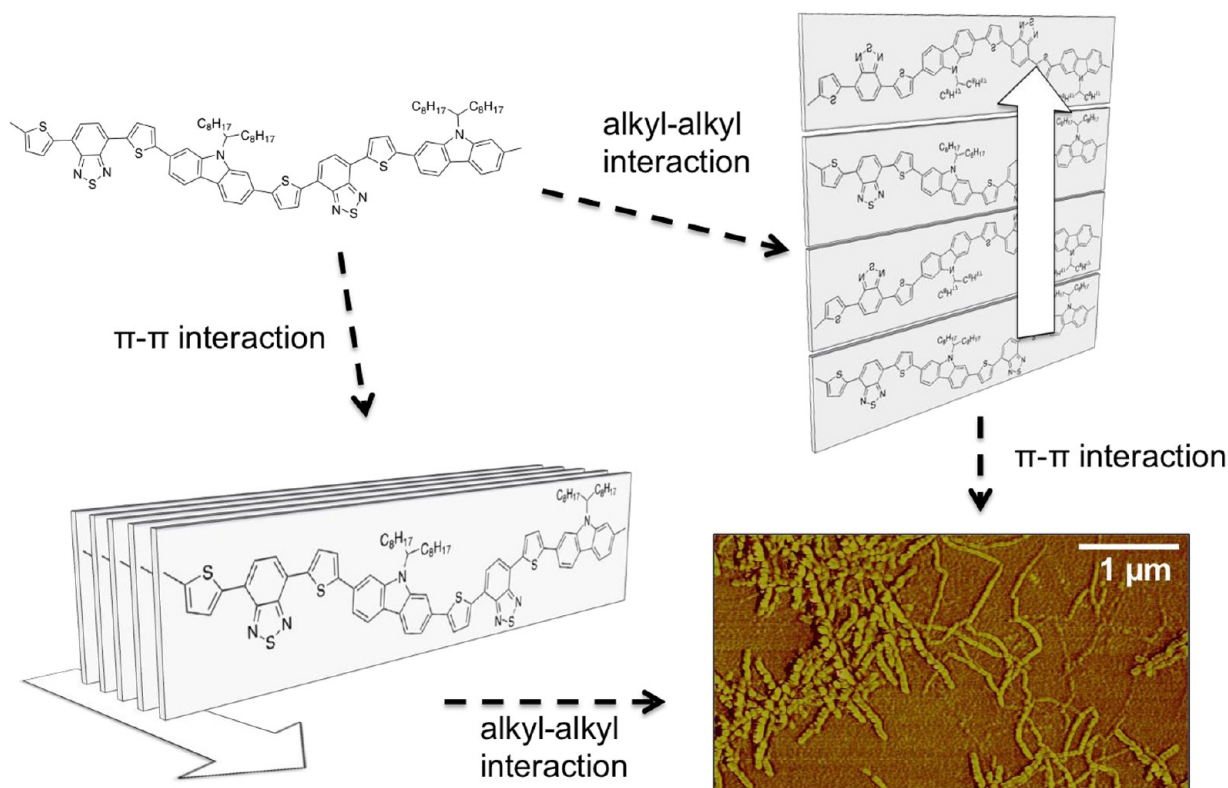


**Figure 2.** Chemical structure of PCDTBT and the proposed schematic of its assembly by a combination of  $\pi$ - $\pi$  stacking and alkyl-alkyl interactions to give the undulated fibril structure observed by AFM.

samples were prepared, and the number-average molecular weights ( $M_n$  values) of the products were estimated by gel permeation chromatography (GPC) performed at 135 °C with trichlorobenzene as the mobile phase and using polystyrene calibration standards.<sup>24</sup> One of the samples had an estimated number-average molecular weight,  $M_n$  of 25.6 kDa with a dispersity ( $\bar{D}$ ) of 1.5, and a second was characterized to have  $M_n$  of 60.1 kDa with  $\bar{D}$  of 1.5. Attempts to form PCDTBT

fibrils using protocols established for P3HT were unsuccessful (see Supporting Information). For example, PCDTBT was dissolved in a marginal solvent, such as anisole, at elevated temperatures, and the solution was allowed to cool slowly. Alternatively, PCDTBT was first dissolved in a good solvent, such as chloroform, followed by addition of a marginal solvent, like anisole. In each case, random aggregates or featureless structures were observed by electron microscopy (see Figure

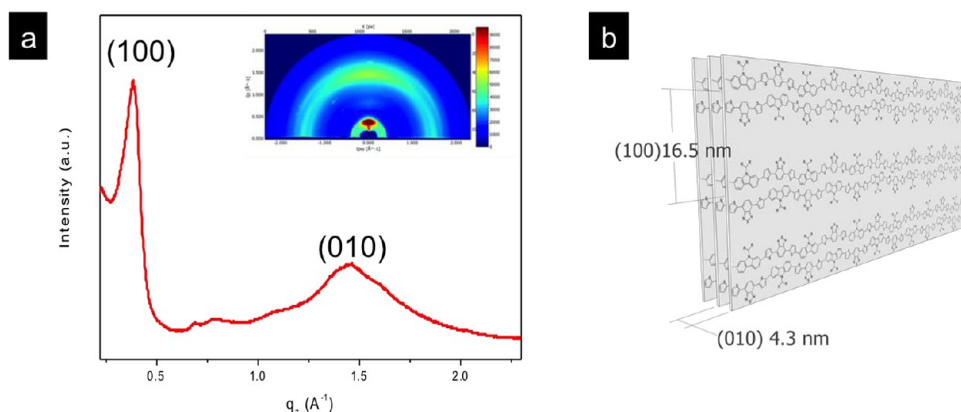


**Figure 3.** (a) GI-WAXS patterns (inset) and integrated 1-D profiles of drop casted films of PCDTBT fibers and (b) the corresponding crystal lattice.

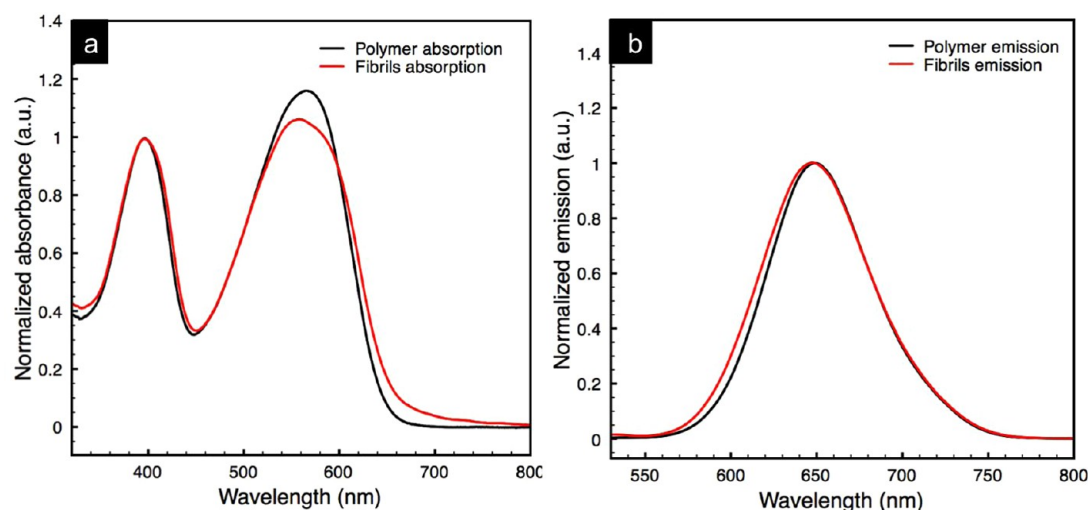


**Figure 4.** (a) Solution UV-vis absorption spectra of PCDTBT fibrils (red) and PCDTBT polymer (black) normalized to higher energy band and (b) normalized fluorescence emission spectra of PCDTBT fibrils (red) and PCDTBT polymer (black).

SI-2). PCDTBT fibers were ultimately obtained by heating the polymer in a marginal solvent (dichloromethane) at elevated temperatures in a sealed vessel (see SI for experimental details).

The influence of processing on the morphology of PCDTBT was characterized by drop-casting the dichloromethane solution onto a carbon-coated grid for characterization by transmission electron microscopy (TEM). TEM images showed individual PCDTBT fibril-like structures, having widths  $\sim 40$ – $60$  nm and lengths  $\sim 0.5$   $\mu\text{m}$  (Figure 1a). The truncated lengths of these PCDTBT fibrils relative to P3HT fibrils ( $\sim 0.5$   $\mu\text{m}$  vs multiple micrometers) suggest that the interchain packing is less well-defined or that multiple nucleation sites are present, preventing the formation of extended (micrometer length) structures. Attempts to form fibrils from the higher molecular weight sample of PCDTBT ( $M_n = 60.1$  kDa) using the same protocol were unsuccessful.

Further characterization of these PCDTBT nanostructures by atomic force microscopy (AFM) indicated that the dominant morphology consists of fibrillar structures  $60$ – $80$  nm in width (Figure 1b,c), values slightly larger than those obtained by TEM, presumably due to the edge effect of the AFM probe. Interestingly, both height and phase images under tapping mode showed these fibers are composed of substructures,<sup>25</sup> implying that the fibrillar structure consists of smaller crystalline units. Annealing the fibers at  $260$   $^{\circ}\text{C}$  ( $\sim 10$

$^{\circ}\text{C}$  above melting point of PCDTBT) led to the disappearance of these granular substructures (see Figure SI-5), similar to what has been observed for polymers such as syndiotactic polypropylene<sup>26</sup> and polyethylene.<sup>27</sup> The substructured nature of the PCDTBT fibrils suggests the assembly of individual PCDTBT chains into crystallites, either by  $\pi$ – $\pi$  stacking or alkyl–alkyl interactions (Figure 2), which further assemble, possibly by preferential interactions of different surfaces of the crystallites, to give the undulated fibrillar structures seen by AFM.

To study the growth mechanism of PCDTBT fibers, we sampled the solution at different time intervals after quenching to room temperature (Figure SI-6). TEM performed on a sample taken 3 min after quenching showed the presence of two types of structures, one  $10 \times 50$   $\text{nm}^2$  and the other  $40 \times 40$   $\text{nm}^2$ . TEM of samples taken 24 h after quenching show that these smaller structures disappear, and the fibrils shown in Figure 1a become the dominant species, suggesting assembly of smaller crystallite structures into the observed fibrils. Ongoing studies aim to better understand the formation of the smaller subunits and their assembly into the bulk crystalline fibrils.

GI-WAXS characterization of the PCDTBT fibrils examined their crystallinity and polymer chain ordering (Figure 3). (h00) and (010) reflections were seen along the  $q_z$  (out-of-plane) axis, giving an interchain separation distance of  $16.5$   $\text{\AA}$  ( $0.38$   $\text{\AA}^{-1}$ ),



characteristic of the alkyl side chain packing; an interchain  $\pi$ – $\pi$  stacking distance of 4.3 Å (1.46 Å<sup>–1</sup>) was also observed. These distances are comparable to those in thermally annealed films of PCDTBT.<sup>20</sup>

If the polymer chains in PCDTBT fibrils are stacked and oriented perpendicular to the fibril axis, as in P3HT fibers, then the fiber width of 40–60 nm observed by TEM would correspond to approximately 20–30 repeat units of PCDTBT (given a repeat unit length  $\sim$ 2 nm).<sup>20</sup> SEC results for these PCDTBT samples suggested a higher DP ( $\sim$ 35 or 25.6 kDa), a reasonable estimate given that the molecular weight of conjugated polymers of this type will be overestimated by SEC.<sup>28</sup> If the substructures are single crystalline and the  $\pi$ – $\pi$  stacking direction is along the fibril axis, then the height of these modular features will correspond to an integral number of (100) planes. With this in mind, the height and length of the crystalline subunits comprising the fibrils are dictated by the relative rates of crystallization along the (100) and (010) directions, respectively, and fibril width is determined by the lengths of the PCDTBT chains.

Characterization of PCDTBT fibrils by absorption and fluorescence emission spectroscopy showed little change between the solvated polymer and the fibrils (Figure 4). This stands in marked contrast to the changes in absorption spectra observed upon P3HT fibril formation, where the absorption maximum exhibits a significant red shift of  $>50$  nm, with the appearance of vibronic bands in place of a featureless solution spectrum.<sup>9</sup> The fluorescence emission spectrum of PCDTBT fibrils shows essentially no change compared to the solvated polymer. In crystalline P3HT, strong intrachain and interchain electronic couplings produce the spectral changes relative to solvated polymer; hence, the lack of significant spectral signatures of the PCDTBT fibrils implies that  $\pi$ – $\pi$  stacking and alkyl–alkyl interactions in these crystals have little influence on the electronic structure within the polymer chains or between neighboring chains. Moreover, it should be noted that P3HT contains only one vibronic band, while PCDTBT has over 15;<sup>29,30</sup> thus, if vibronic bands do appear upon PCDTBT crystallization, their overlapping nature may lead to a featureless spectrum. The lack of a spectroscopic signature in the absorption spectrum further reflects the uniqueness of P3HT from these low band gap polymer structures. We are currently probing the photophysical characteristics of the PCDTBT crystals using single molecule techniques to determine the exact nature of intra- and interchain coupling and remove any possible effects of residual free (nonfibril) polymer.

In summary, we have developed a simple solution-based method to prepare crystalline fibrillar structures from the low band gap polymer PCDTBT. These structures have widths of 40–60 nm and lengths of  $\sim 0.5$   $\mu$ m, as determined by TEM, and their crystallinity was confirmed by GI-WAXS. AFM revealed that the fibrils have a textured structure, and time-dependent studies of crystal growth suggest smaller subunits assemble, with crystallization occurring through  $\pi$ – $\pi$  and alkyl–alkyl interactions. Interestingly, no distinct spectroscopic signatures in either absorption or fluorescence emission were detected upon PCDTBT fibrillization, suggesting that little change in electronic coupling between neighboring chains occurs upon crystallization. This solution-based assembly of the low band gap polymer PCDTBT into fibrillar structures offers new insight into structure–property relationships of conjugated polymers, ultimately benefitting the design of novel polymeric

materials for solar cells and other applications of conjugated polymer materials.

## ■ ASSOCIATED CONTENT

### Supporting Information

Detailed materials characterization methods and instrumentation. This material is available free of charge via the Internet at <http://pubs.acs.org>.

## ■ AUTHOR INFORMATION

### Corresponding Author

\*E-mail: [russell@mail.pse.umass.edu](mailto:russell@mail.pse.umass.edu); [tsemrick@mail.pse.umass.edu](mailto:tsemrick@mail.pse.umass.edu).

### Present Address

<sup>†</sup>Department of Chemistry, Case Western Reserve University, Cleveland, OH 44106–7078 (E.P.)

### Notes

The authors declare no competing financial interest.

## ■ ACKNOWLEDGMENTS

This work was supported by the Department of Energy supported Energy Frontier Research Center at the University of Massachusetts (DE-SC0001087), and facilities of the NSF-supported Materials Research Science and Engineering Center at the University of Massachusetts (DMR-0820506). We thank J. Lawrence and A. Wise for helpful discussions. Portions of this research were carried out at the Stanford Synchrotron Radiation Laboratory, a national user facility operated by Stanford University on behalf of the U.S. Department of Energy, Office of Basic Energy Sciences.

## ■ REFERENCES

- (1) Liu, F.; Gu, Y.; Jung, J. W.; Jo, W. H.; Russell, T. P. *J. Polym. Sci., Part B: Polym. Phys.* **2012**, *50*, 1018–1044.
- (2) Dayal, S.; Kopidakis, N.; Olson, D. C.; Ginley, D. S.; Rumbles, G. *Nano Lett.* **2010**, *10*, 239–242.
- (3) Sirringhaus, H.; Brown, P. J.; Friend, R. H.; Nielsen, M. M.; Bechgaard, K.; Langeveld-Voss, B. M. W.; Spiering, A. J. H.; Janssen, R. A. J.; Meijer, E. W.; Herwig, P.; de Leeuw, D. M. *Nature* **1999**, *401*, 685–688.
- (4) Liu, F.; Gu, Y.; Wang, C.; Zhao, W.; Chen, D.; Briseno, A. L.; Russell, T. P. *Adv. Mater.* **2012**, *24*, 3947–3951.
- (5) Collins, B. A.; Li, Z.; Tumbleston, J. R.; Gann, E.; McNeill, C. R.; Ade, H. *Adv. Energy Mater.* **2012**, *3*, 65–74.
- (6) Li, G.; Shrotriya, V.; Huang, J.; Yao, Y.; Moriarty, T.; Emery, K.; Yang, Y. *Nat. Mater.* **2005**, *4*, 864–868.
- (7) Kim, F. S.; Ren, G.; Jenekhe, S. A. *Chem. Mater.* **2011**, *23*, 682–732.
- (8) Wu, P.-T.; Xin, H.; Kim, F. S.; Ren, G.; Jenekhe, S. A. *Macromolecules* **2009**, *42*, 8817–8826.
- (9) Berson, S.; De Bettignies, R.; Bailly, S.; Guillerez, S. *Adv. Funct. Mater.* **2007**, *17*, 1377–1384.
- (10) Kim, J.-H.; Park, J. H.; Lee, J. H.; Kim, J. S.; Sim, M.; Shim, C.; Cho, K. J. *Mater. Chem.* **2010**, *20*, 7398–7405.
- (11) Pentzer, E. B.; Bokel, F. A.; Hayward, R. C.; Emrick, T. *Adv. Mater.* **2012**, *24*, 2254–2258.
- (12) Ren, S.; Chang, L.-Y.; Lim, S.-K.; Zhao, J.; Smith, M.; Zhao, N.; Bulović, V.; Bawendi, M.; Građević, S. *Nano Lett.* **2011**, *11*, 3998–4002.
- (13) Bokel, F. A.; Sudeep, P. K.; Pentzer, E.; Emrick, T.; Hayward, R. C. *Macromolecules* **2011**, *44*, 1768–1770.
- (14) Hammer, B. A. G.; Bokel, F. A.; Hayward, R. C.; Emrick, T. *Chem. Mater.* **2011**, *23*, 4250–4256.
- (15) Samitsu, S.; Shimomura, T.; Ito, K. *Thin Solid Films* **2008**, *516*, 2478–2486.

- (16) Grenier, C. R.; Pisula, W.; Joncheray, T. J.; Müllen, K.; Reynolds, J. R. *Angew. Chem., Int. Ed.* **2007**, *46*, 714–717.
- (17) Park, S. H.; Roy, A.; Beaupré, S.; Cho, S.; Coates, N.; Moon, J. S.; Moses, D.; Leclerc, M.; Lee, K.; Heeger, A. J. *Nat. Photonics* **2009**, *3*, 297–302.
- (18) Peters, C. H.; Sachs-Quintana, I. T.; Kastrop, J. P.; Beaupré, S.; Leclerc, M.; McGehee, M. D. *Adv. Energy Mater.* **2011**, *1*, 491–494.
- (19) Sun, Y.; Takacs, C. J.; Cowan, S. R.; Seo, J. H.; Gong, X.; Roy, A.; Heeger, A. J. *Adv. Mater.* **2011**, *23*, 2226–2230.
- (20) Lu, X.; Hlaing, H.; Germack, D. S.; Peet, J.; Jo, W. H.; Andrienko, D.; Kremer, K.; Ocko, B. M. *Nat. Commun.* **2012**, *3*, 795.
- (21) Wang, T.; Pearson, A. J.; Dunbar, A. D.; Staniec, P. A.; Watters, D. C.; Yi, H.; Ryan, A. J.; Jones, R. A.; Iraqi, A.; Lidzey, D. G. *Funct. Mater.* **2012**, *22*, 1321.
- (22) Beiley, Z. M.; Hoke, E. T.; Noriega, R.; Dacuña, J.; Burkhard, G. F.; Bartelt, J. A.; Salleo, A.; Toney, M. F.; McGehee, M. D. *Adv. Energy Mater.* **2011**, *1*, 954–962.
- (23) Blouin, N.; Michaud, A.; Leclerc, M. *Adv. Mater.* **2007**, *19*, 2295–2300.
- (24) Blouin, N.; Michaud, A.; Gendron, D.; Wakim, S.; Blair, E.; Neagu-Plesu, R.; Belletête, M.; Durocher, G.; Tao, Y.; Leclerc, M. *J. Am. Chem. Soc.* **2008**, *130*, 732–742.
- (25) Ouhib, F.; Desbief, S.; Lazzaroni, R.; De Winter, J.; Gerbaux, P.; Jérôme, C.; Detrembleur, C. *Macromolecules* **2012**, *45*, 6796–6806.
- (26) Heck, B.; Hugel, T.; Iijima, M.; Sadiku, E.; Strobl, G. *New J. Phys.* **1999**, *1*, 17.
- (27) Loos, J.; Thüne, P. C.; Niemantsverdriet, J. W.; Lemstra, P. J. *Macromolecules* **1999**, *32*, 8910–8913.
- (28) Liu, J.; Loewe, R. S.; McCullough, R. D. *Macromolecules* **1999**, *32*, 5777–5785.
- (29) Reish, M. E.; Nam, S.; Lee, W.; Woo, H. Y.; Gordon, K. C. *J. Phys. Chem. C* **2012**, *116*, 21255–21266.
- (30) Banerji, N.; Gagnon, E.; Morgantini, P.-Y.; Valouch, S.; Mohebbi, A. R.; Seo, J. H.; Leclerc, M.; Heeger, A. J. *J. Phys. Chem. C* **2012**, *116*, 11456–11469.